

HEAT TRANSFER FROM FINNED SURFACE IN DOWNWARD-FACING SUBCOOLED FLOW BOILING

Abdul R. Khan, Nejdet Erkan, Koji Okamoto

Department of Nuclear Engineering and Management, University of Tokyo

7-3-1 Hongo, Bunkyo-ku, Tokyo 113-8656, Japan

khan@vis.t.u-tokyo.ac.jp, erkan@vis.t.u-tokyo.ac.jp, okamoto@n.t.u-tokyo.ac.jp

ABSTRACT

Severe Accident Management Guidelines exist to mitigate the effects of severe accidents. A particular strategy that may prevent RPV failure for PWRs is In-vessel Retention (IVR). During IVR, a large amount of heat may be transferred to the water from the vessel surface. If excessive boiling conditions are reached, Critical Heat Flux (CHF) conditions may occur. Therefore, increasing the safety margin for the CHF limit is an important aspect that should be considered especially for future larger-power Light Water Reactors. Although many different enhancement techniques may be available, a simple method of enhancing heat transfer can be performed through fins. Therefore, an experimental study was performed to investigate the heat transfer effect from a pin fin during flow boiling conditions. The finned surface was compared to a bare surface in order to observe any effects in the heat transfer. The experiments were performed for different mass flux: 244 kg/m²-s, 215 kg/m²-s, and 177 kg/m²-s. CHF conditions occurred at the lowest flow rate. Results showed the finned surface was able to enhance the heat transfer for 244 kg/m²-s case. The ability of the fin to enhance the heat transfer reduced as CHF conditions were approached. Upstream and downstream temperatures on the finned surface varied, and a significant rise in the downstream temperatures was observed as the flow rate was reduced. Bubble accumulation was also observed downstream after the fin. In some cases the bubble accumulation occurred for a relatively long period, posing a potential risk for the heat transfer.

KEYWORDS

Heat Transfer, Fin, Flow Boiling

1. INTRODUCTION

Recently, focus has been centered on enhancing the safety level required during severe accidents. Procedures part of the Severe Accident Management Guidelines (SAMG) are being incorporated in existing and new reactor designs to strengthen or improve safety systems in nuclear reactors. Accident management strategies as part of SAMGs are expected to mitigate the effects of severe accidents or control the progression of the accident. For example, next generation nuclear reactors are incorporating passive safety systems in their designs. While it may not be for long periods, the passive systems are designed to work without any operator action required. Also, no electrical power is needed for the continuous usage of passive systems for a certain amount of time. Employing such systems will allow for water to be supplied by gravity at the necessary location, or the system may assist in removing heat by natural circulation. If passive safety systems are implemented during severe accidents, they may be able to provide valuable time during which longer-lasting water systems can be applied.

It is vital to retain the fission products released from melting of fuel during a severe accident. If the fission products are released from the Reactor Pressure Vessel (RPV) they can migrate into the containment building, and may eventually escape into the environment. Since this is highly undesired, preventing RPV failure is important during severe accident conditions. This can be achieved by ensuring the integrity of the RPV. A particular severe accident management strategy that may prevent the RPV failure is In-Vessel Retention (IVR) [1,2]. IVR is accomplished by ex-vessel cooling. Once the reactor cavity area is flooded heat is transferred from the vessel surface, reducing the temperature of the RPV lower head. IVR is expected to prevent failure of the RPV wall from overheating.

IVR has been established for the AP600 and AP1000 Light Water Reactors (LWR) [1,3]. Some next generation reactors are designed to output larger power compared to the AP-1000. Current IVR capability may not be applicable for larger-powered reactors. During IVR, decay heat generated by the melted fuel is transferred to the water through the RPV wall. As the heat flux supplied to the water increases, boiling will initiate on the outer surface of the vessel. If excessive boiling conditions occur, the heat flux on the vessel surface may reach Critical Heat Flux (CHF) conditions. CHF is the condition at which even a small amount of additional heat flux will cause a sudden increase in temperatures on the surface. The surface may become damaged due to high surface temperatures and RPV failure may occur. Therefore, it is important to increase the CHF safety margin for future larger-powered LWRs [4-6].

One method to increase the heat transfer from the vessel can be performed by applying a structured design on the vessel surface. Thus, an experimental study was performed to evaluate the heat transfer effect from structured surfaces during flow boiling conditions. While many types of structured surface designs can be considered one of the most basic heat transfer enhancement surfaces is the fin, which is one of the surfaces considered in this study. Even though many studies have been performed on fin heat transfer in the past, studies relating to fin heat transfer in flow boiling conditions have not been found in the literature. As a result, no quantitative data is available to show the effect of the heat transfer from a finned surface during forced convection boiling conditions. Therefore, this preliminary study will provide a better understanding on the boiling phenomenon for such type of geometry. The knowledge obtained will be applied in future experiments in which the same phenomenon will be investigated under saturated conditions. Important aspects relevant to heat transfer and boiling are evaluated from the results of this study.

2. EXPERIMENTAL WORK

2.1. Experimental Apparatus

A small scale experiment was performed to study heat transfer from a finned surface, considering a simple pin fin (cylindrical) design. The preliminary experiments performed in this study focused on downward-facing subcooled flow boiling, which occurred on the bottom surface of a copper block. Performing similar experiments at different angular positions will be considered as future work. The flow loop consisted of a water tank, pump, flow meter, upstream buffer tank, flow channel, and test section (Fig. 1). The test section comprised of the two different surfaces. Two copper blocks had similar designs except for the boiling surface. One block was designed with a bare surface and the other with a pin fin located in the center. It was essential to compare results from both surfaces to observe the effect of the fin. The finned test section is shown in Fig. 2. The bottom surface for both copper blocks was circular in shape with a diameter of 0.02m. The fin dimensions were 0.004m in diameter and extended 0.01m from the center of the surface. The top portion of the block was used to insert five cartridge heaters, each heater rated at 225W. The copper block was insulated with PEEK (polyether ether ketone) to reduce heat loss. Only the bottom portion of the copper block and insulation were exposed to the fluid.

Thermocouples were inserted near the bottom portion of the copper blocks (Fig. 2). The thermocouples provided data required for surface temperature and heat flux calculations. The thermocouple distance was set at 0.004m from the boiling surface. The same distance was also used between consecutive thermocouples. Three thermocouples measured the temperatures in the center of the bare copper block. On the other hand, the location of the fin would not allow for the calculation of the surface temperature and heat flux in the center of the block. As a result, the thermocouples were kept at a location of 4 mm from the outer edge (close to PEEK) of the lower cylindrical region of the block.

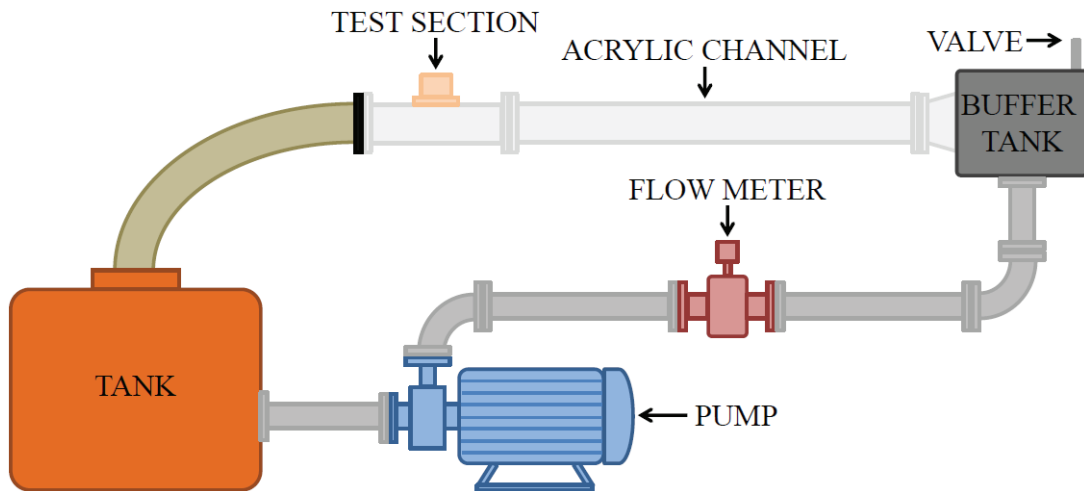


Figure 1: Schematic diagram of the experimental loop.

The water temperature and pressure in the experiments was room temperature and atmospheric pressure, respectively. Different mass flux were applied in the experiments: $244 \text{ kg/m}^2\text{-s}$, $215 \text{ kg/m}^2\text{-s}$, and $177 \text{ kg/m}^2\text{-s}$. The highest flow rate was initially applied, but was reduced in order to reach CHF conditions. CHF was observed only for the lowest flow rate.

Visualization of both block types was also performed for qualitative analysis of the boiling process. In the experiments, images were recorded while viewing the surface from below the channel. A high speed high resolution camera was utilized for the visualization of the experiments. The resolution and recording speed were chosen to be 1024 pixels x 1024 pixels and 1000 frames per second, respectively.

2.2 Experimental Procedure

Prior to performing the experiments, the boiling surface was polished and cleaned with acetone before placing it in the channel. The boiling experiments began when the desired flow rate and steady state flow conditions were achieved. The power supplied to the heaters was controlled by a variable transformer. The voltage ranged from 0 to 240V, with 240V providing maximum power to the heaters. From previous trial experiments, a range of 120V to 220V was adequate for both copper blocks. Due to the possibility of damaging the insulation, maximum power was not applied.

The first voltage level applied was 120V, and the following levels were incremented in intervals of 10V until 220V. After the voltage was applied, steady state temperatures were measured before proceeding to the next voltage. The video observations of the boiling phenomenon were performed during the steady state period. The voltage was increased to the next level, steady state temperatures were observed, and the voltage was increased again. This process continued until all voltage levels were completed. All experiments were repeated twice for repeatability purposes, and the averaged results are presented.

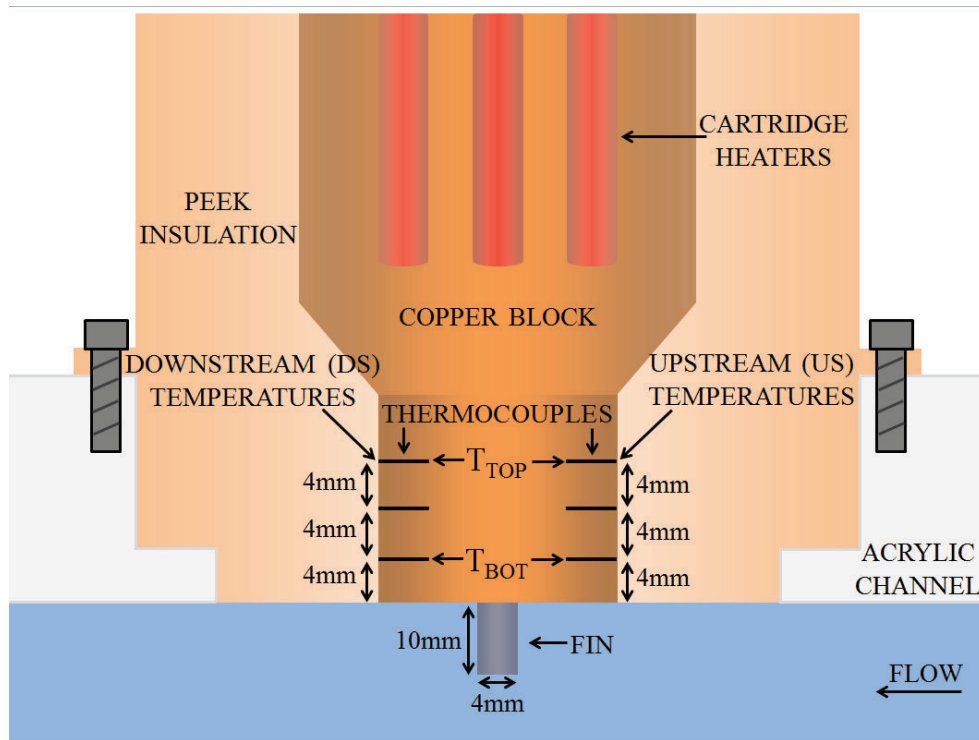


Figure 2: Schematic diagram of the finned surface test section.

2.3 Data Analysis

The thermocouples provided temperature data for the surface temperature and heat flux calculations. The measurement uncertainty of the K-type thermocouples was 0.75% of the measured value. Steady state temperature data obtained after voltage adjustment was used to calculate the average temperature at each thermocouple location. Only the time-averaged data resulting in a standard deviation of 0.5 °C or less was used for the surface temperature calculation (T_s , °C), given by

$$T_s = T_{bot} + \frac{1}{2}(T_{bot} - T_{top}) \quad (1)$$

where T_{bot} (°C) is the temperature of the thermocouple closest to the boiling surface and T_{top} (°C) is the temperature of the thermocouple farthest from the boiling surface (Fig. 2). The middle thermocouple between T_{top} and T_{bot} was used as a means of verifying the linearity of the temperature profile. The temperatures given by equation (1) were compared with temperatures calculated from the least squares

method using all three thermocouples. Both set of temperatures were found to be quite similar. The average thermocouple temperatures were also used to calculate the surface heat flux by assuming 1-D conduction as the main mechanism of heat transfer to the boiling surface. The 1-D conduction assumption was confirmed by the linear temperature profile of the thermocouple data at the three different locations. An approximate average surface heat flux (q'' , MW/m²) was estimated by

$$q'' = k \frac{\Delta T}{\Delta x} = k \frac{T_{top} - T_{bot}}{\Delta x} \quad (2)$$

with k (391 W/m-K) as the thermal conductivity of copper and Δx (0.008m) as the distance between T_{top} and T_{bot} . The surface temperature and heat flux for the different voltages were used to create boiling curves. The results are presented in the following sections. Note that the surface temperature and heat flux are local estimations.

A simple calculation for the local heat transfer coefficient was performed by using Newton's law of cooling,

$$q'' = h \Delta T = h (T_s - T_{film}) \quad (3)$$

where q'' is the surface heat flux calculated by Eq. (2) and T_{film} (°C) is the film temperature i.e. the average temperature between T_s and the bulk water temperature. Rearranging Eq. (3), the local experimental heat transfer coefficient (h_{exp} , W/m²-K) was given by

$$h_{exp} = \frac{q''}{(T_s - T_{film})} \quad (4)$$

Again, the heat transfer coefficient in Eq. (4) is a local value and should not be taken as the overall heat transfer coefficient.

3. RESULTS & DISCUSSION

3.1 Boiling Curves

The boiling curves were obtained for bare and finned surfaces. For convenience, 244 kg/m²-s will be referred to as the high flow rate, 215 kg/m²-s as the medium flow rate, and 177 kg/m²-s as the low flow rate. CHF conditions were observed only for the low flow rate. Since the voltage level at which CHF occurred was lower, fewer data points are presented for the low flow rate.

The emphasis of the results is towards the higher heat flux. Figure 3 shows data separated into the bare and finned surfaces for all three flow rates. Figure 3(A) presents the boiling curves for the bare surface only, whereas Fig. 3(B) presents the boiling curves for the fin-upstream location (thermocouple location before the fin in Fig. 2) and Fig 3(C) presents the boiling curves for the fin-downstream location (thermocouple location after the fin in Fig. 2). In Fig. 3(A) the curves for the high and medium flow rates are quite similar, but the low flow rate shows slightly lower surface temperatures. The fin-upstream location in Fig. 3(B) first shows a reduction in the surface temperatures when the flow rate is reduced from high to medium, and then an increase in the temperatures when the flow rate is reduced further. In Fig. 3(C) the temperatures on the fin-downstream location are decreasing as the flow rate is decreasing. Note that the fin-downstream location temperatures for the medium and low flow rates surpass the bare surface and fin-upstream location temperatures, implying a reduction in the heat transfer for these two flow rates.

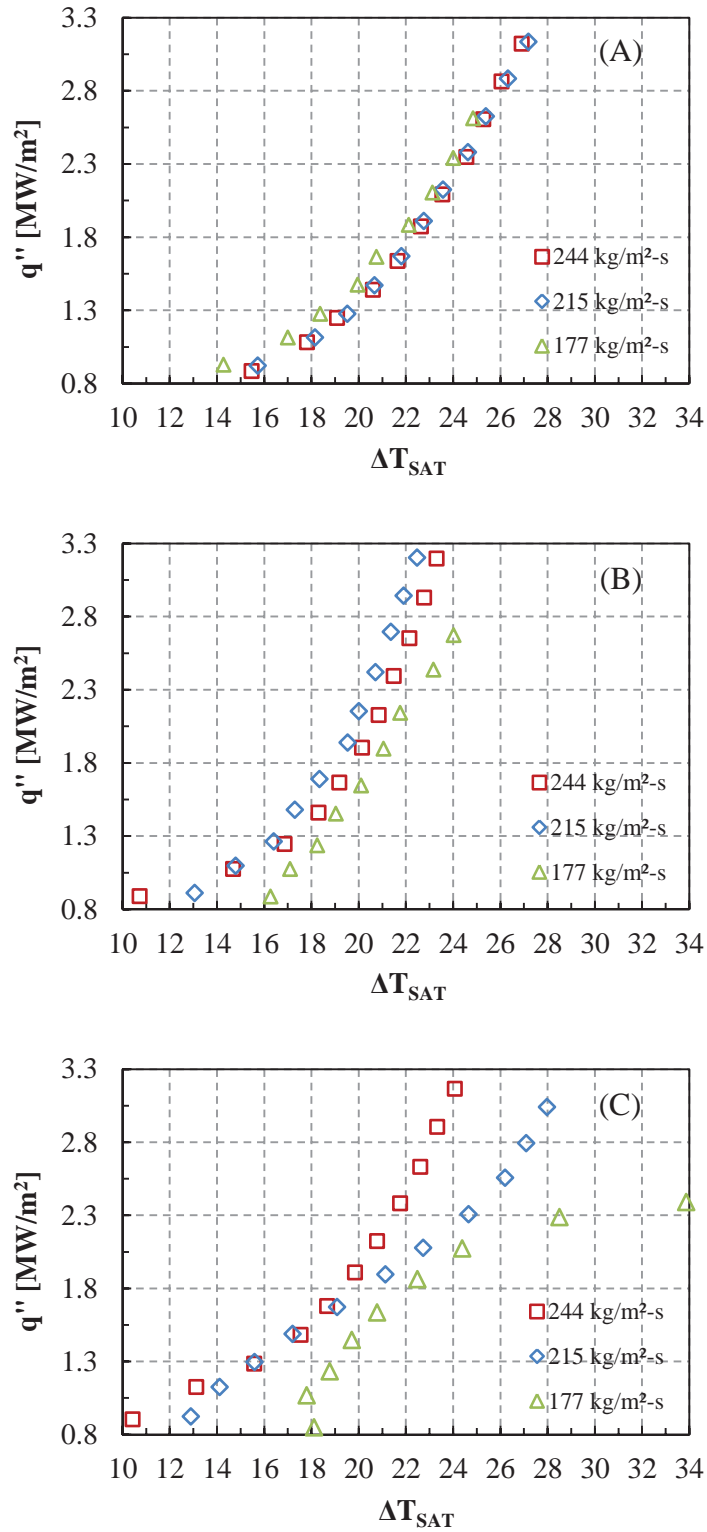


Figure 3: Boiling curves for the bare and finned surfaces: (A) bare surface, (B) upstream location on finned surface, (C) downstream location on finned surface.

As mentioned earlier, CHF (Fig. 4) was observed for the lowest flow rate. The data point at the highest heat flux for $177 \text{ kg/m}^2\text{-s}$ in Fig. 3 is the CHF value. CHF was defined as the moment when the bubble covered the entire boiling surface, causing a rapid increase in the thermocouple temperature inside the copper blocks. Note that only the portion of the fin base close to the boiling surface was covered by the bubble, and not the entire fin along its length.

The manner in which CHF occurred will be briefly described. Upon reaching the voltage level at which CHF was observed, the boiling on the surface remained similar as was observed in the preceding voltage level. Intermittently, there was a large bubble that appeared suddenly downstream. After a relatively short period, the large bubble would be removed from the surface. Immediately before CHF occurred, the large bubble formed downstream and increased in size as the bubble front slowly covered more of the boiling surface while moving upstream. An oscillatory motion of the bubble front was observed. As the bubble front moved upstream to cover the whole surface, it did so for a moment and was pushed back. This oscillating motion continued until after some time the whole surface was covered by the bubble (Fig. 4).

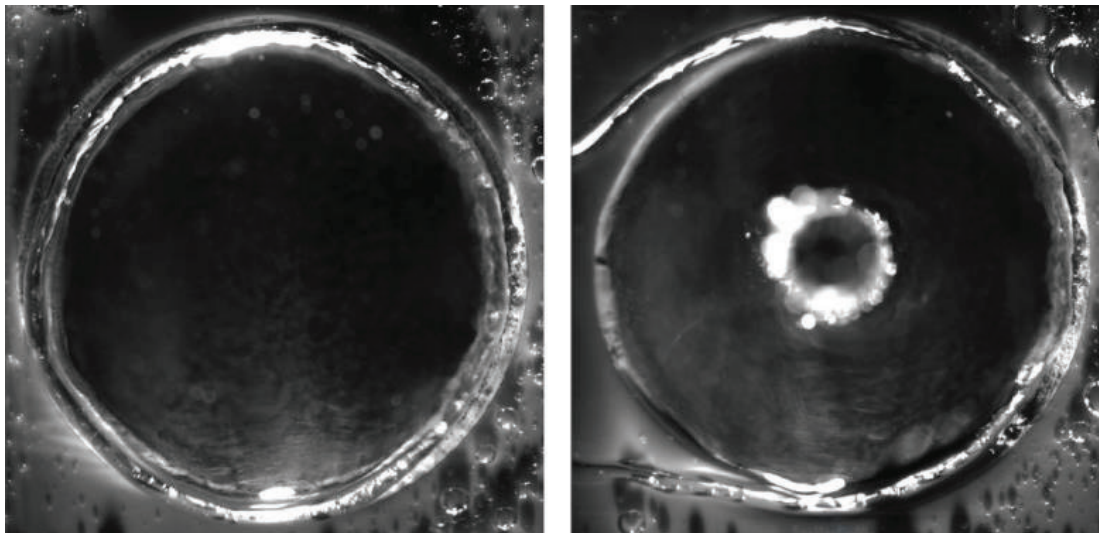


Figure 4: CHF at $177 \text{ kg/m}^2\text{-s}$ on both surfaces: left) bare surface, right) finned surface.

3.2 Heat Transfer

In order to observe effects in the heat transfer due to the addition of the fin, the relative enhancement is shown in Fig. 5 for all three flow rates. The enhancement due to the fin is shown relative to the bare surface, using the heat transfer coefficients calculated for both surfaces. The relative enhancement was defined as the difference between the finned heat transfer coefficient and the bare heat transfer coefficient, divided by the latter. The relative enhancement in Fig. 5 is shown for the upstream (US) and downstream (DS) locations on the finned surface. Again, the emphasis of the results is towards higher heat flux. Values above 0 imply improvement in the heat transfer on the finned surface relative to the bare surface.

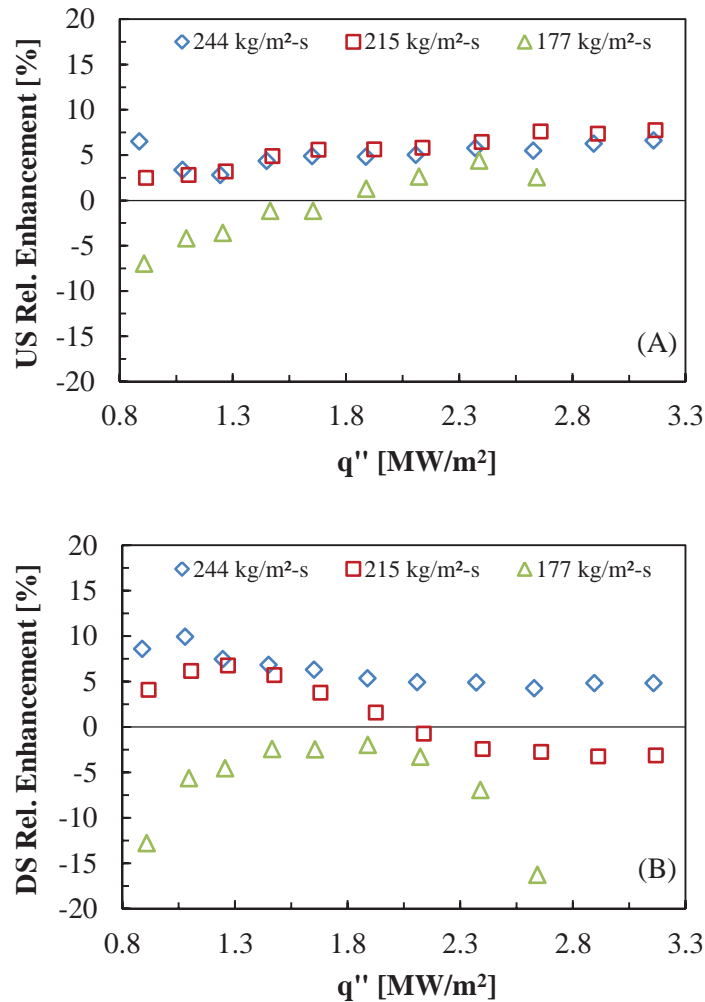


Figure 5: Relative enhancement for the finned surface: (A) fin-upstream (US) location, (B) fin-downstream (DS) location.

In Fig. 5(A) the value is greater than 0 for the high and medium flow rates, implying improvement in the heat transfer for the fin-upstream location. The low flow rate initially shows a value below 0, but increases as the heat flux increases. An overall improvement in the heat transfer is observed for the fin-upstream location. On the other hand, Fig. 5(B) shows improvement only for the high flow rate. A transition from improvement to reduction of the heat transfer occurs for the medium flow rate. For the low flow rate case the value starts to increase, but reduces as the heat flux increases to CHF. The low flow rate does not show any improvement in the heat transfer, as the value is below 0 for all heat flux. In Fig. 5(B), a reduction in the heat transfer is observed as the flow rate is reduced.

The heat transfer for the fin-downstream location has been enhanced locally for the high flow rate, but the heat transfer reduction is increasing as the flow rate decreases i.e. the difference in the values between each flow rate is increasing (at higher heat flux) as the flow rate is decreasing. The addition of a fin usually enhances the heat transfer, but a reduction in the local heat transfer is found in this study.

The heat transfer reduction may occur due to bubble accumulation after the fin (Fig. 6). The accumulation may cause increase in temperatures for the fin-downstream location. There is no obstruction in the flow path for the fin-upstream location, so the liquid is able to contact the heated surface directly. For the fin-downstream location, the flow is affected due to the fin. The flow can be described as for a cylinder in cross-flow. A wake is produced downstream as the flow passes the cylinder. Since boiling is also occurring during the experiments, the bubbles will be entrained in the flow and accumulate in the wake. In some cases, the bubble remains on the surface for a significant amount of time. Furthermore, the liquid velocity is reduced considerably compared to the bulk flow in the wake region [7]. The bubble accumulation and lower velocity in the fin-downstream location will affect the heat transfer. The accumulation will reduce the liquid contact with the surface and the low velocity will decrease the general heat transfer. The bubble accumulation may pose a risk, as it may cause a hotspot at that location i.e. the temperatures may increase rapidly for the given duration the bubble remains on the surface. The reduced velocities and bubble accumulation in the wake region are believed to have caused the rise in fin-downstream location temperatures and the reduction in the heat transfer.

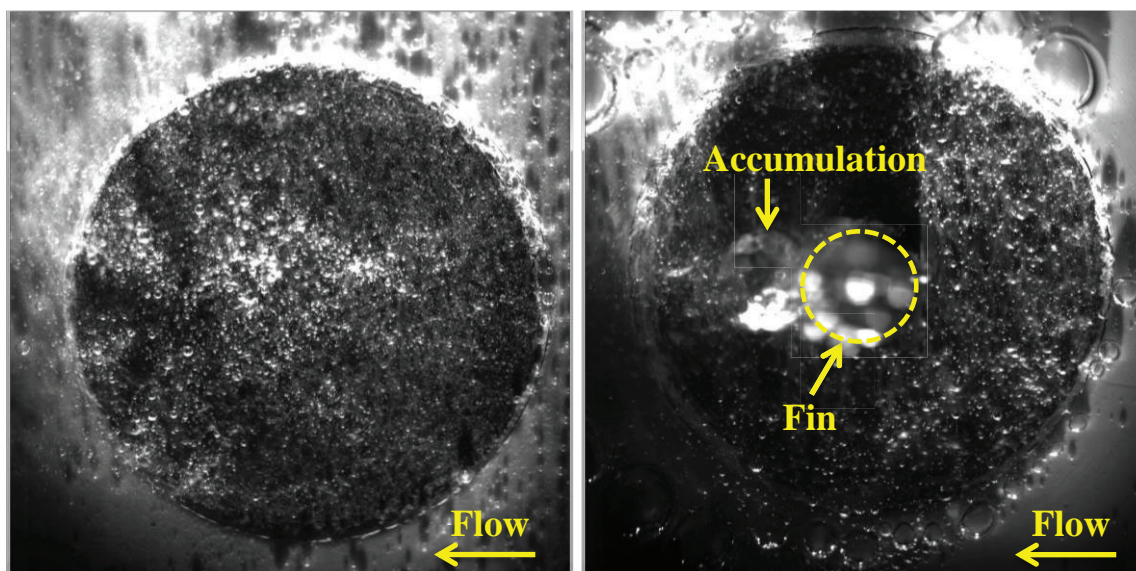


Figure 6: Comparison of bare (left image) and finned surfaces (right image), showing the bubble accumulation after the fin.

4. CONCLUSIONS

IVR may be an effective method to insure the integrity of the RPV during severe accident conditions. Although it has been established for the AP1000 reactor, it may not be capable of performing ex-vessel cooling sufficiently for larger-powered reactors. Another method should be considered for preventing failure and ensuring the integrity of the RPV. A simple method to enhance heat transfer from a surface can be performed by fins. Therefore, an experiment was performed to assess the fundamentals of heat transfer from a finned surface in downward-facing subcooled flow boiling. Studies related to finned surface effects in flow boiling were not found in the literature, and no quantitative data was available to show the effect of the heat transfer from a finned surface during forced convection boiling conditions. A comparison between bare and finned surface was performed to evaluate effects of heat transfer from the latter. The following are the main conclusions from this work:

- finned surface is able to enhance heat transfer in subcooled flow boiling conditions
- ability of fin to enhance heat transfer is greater when conditions are far from CHF
- fin-downstream location temperatures increase significantly as flow rate is reduced
- the wake produced at the fin-downstream location caused bubble accumulation
- a decline in the local heat transfer coefficient for the fin-downstream location was found

In short, local heat transfer reduction has been observed even with the presence of a fin. Furthermore, bubble formation at a specific location for a certain amount of time may cause local hot spots with high surface temperatures, which may lead to a damaged surface. More work is required to assess the effects from finned surfaces in flow boiling conditions. The results from this preliminary work are expected to assist in future experiments where the same phenomenon will be studied at saturated conditions and with a larger range of flow rates. Also, investigating the effect of different angular positions is desired.

REFERENCES

1. J.L. Rempe, D.L. Knudson, C.M. Allison, G.L. Thinnis, C.L. Atwood, M.J. Cebull, "Potential for AP600 In-Vessel Retention through Ex-Vessel Flooding," INEEL/EXT-97-00779, Idaho National Engineering and Environment Laboratory (1997).
2. T.G. Theofanous, C. Liu, S. Additon, S. Angelini, O. Kymalainen, T. Salmassi, "In-vessel coolability and retention of a core melt," *Nuclear Engineering and Design* **169**, pp. 1-48 (1997).
3. T-N. Dinh, J.P. Tu, T. Salmassi, T.G. Thofanous, "Limits of Coolability in the AP1000-Related ULPU-2400 Configuration V Facility," CRSS-03/06 (2003).
4. S.D. Park, I.C. Bang, "Flow boiling CHF enhancement in an external reactor vessel cooling (ERVC) channel using graphene oxide nanofluid," *Nuclear Engineering and Design* **265**, pp. 310-318 (2013).
5. J.L. Rempe and D.L. Knudson, "Margin for In-Vessel Retention in the APR1400 – VESTA and Scdap/Relap5-3D Analyses," INEEL/EXT-04-02549, Idaho National Engineering and Environment Laboratory (2004).
6. J.L. Rempea, D.L. Knudsona, K.G. Condie, K.Y. Suhb, F.-B. Cheung, S.-B. Kim, "Corium retention for high power reactors by and in-vessel core catcher in combination with External Reactor Vessel Cooling," *Nuclear Engineering and Design* **230**, pp. 293-309 (2004).
7. H.M Warui, N. Fujisawa, "Feedback control of vortex shedding from a circular cylinder by cross-flow cylinder oscillations," *Experiments in Fluids* **21**, pp. 49-56 (1996).